JACS Au
AN OPEN ACCESS JOURNAL OF THE AMERICAN CHEMICAL SOCIETY

pubs.acs.org/jacsau

Article

Multi-Reconfigurable DNA Origami Nanolattice Driven by the Combination of Orthogonal Signals

Kotaro Watanabe, Ibuki Kawamata, Satoshi Murata, and Yuki Suzuki*

Cite This: *JACS Au* 2023, 3, 1435−1442

Read Online

ACCESS | Metrics & More | Article Recommendations | Supporting Information

ABSTRACT: The progress of the scaffolded DNA origami technology has enabled the construction of various dynamic nanodevices imitating the shapes and motions of mechanical elements. To further expand the achievable configurational changes, the incorporation of multiple movable joints into a single DNA origami structure and their precise control are desired. Here, we propose a multi-reconfigurable 3 × 3 lattice structure consisting of nine frames with rigid four-helix struts connected with flexible 10-nucleotide joints. The configuration of each frame is determined by the arbitrarily selected orthogonal pair of signal DNAs, resulting in the transformation of the lattice into various shapes. We also demonstrated sequential reconfiguration of the nanolattice and its assemblies from one into another via an isothermal strand displacement reaction at physiological temperatures. Our modular and scalable design approach could serve as a versatile platform for a variety of applications that require reversible and continuous shape control with nanoscale precision.

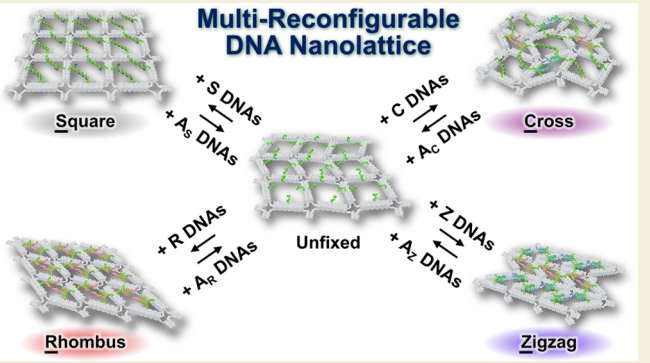

KEYWORDS: *self-assembly, multi-responsivity, reconfiguration, nanodevice, DNA nanotechnology, DNA origami*

INTRODUCTION

Owing to the development of methods to fold DNA into artificial nanostructures and evolution of the chemical synthesis of custom oligonucleotides, DNA is now widely used as a programmable nanomaterial.[1,2] The early stage of the field of the structural DNA nanotechnology focused on the fabrication of static nanostructures with high precision in a robust manner.[3−5] In addition to that methodology, a variety of dynamic DNA nanodevices have been developed based on the differences in physical properties between single-stranded DNA (ssDNA) and double-stranded DNA (dsDNA).[6,7] ssDNA is often regarded as a flexible joint owing to its short persistence length (∼1.3 nm), whereas dsDNA has a persistence length of ∼50 nm[8−10] and is further bundled into rigid parts of the devices. Among the different types of methods implemented in structural DNA nanotechnology, scaffolded DNA origami is a powerful technique to obtain a desired two-/three-dimensional shape[11−14] and thus has been employed to construct reconfigurable nanodevices imitating normal-sized mechanical objects.[15−17] Successful attempts are represented by the development of DNA nanodevices and nanorobots exhibiting open-close motion,[15,18−25] sliding motion,[15,26,27] or rotary motion.[28−33]

One of the most popular strategies for constructing dynamic DNA nanodevices is to design flexible connections such as hinges and joints[15] and install angle-adjustable mechanisms for them.[34,35] Implementing multiple such connections can enhance the complexity of achievable motions of DNA nanodevices. For example, paper-folding-inspired motions were realized by designing six hinges in a DNA origami nanostructure,[36] while kinematic motions were achieved by linking eight-helix bundles with multiple joints.[37] Propagation of conformation change based on mechanical linkage was also exhibited by controlling one of the angles in a rhombus-shaped nanostructure.[38] Besides these scaffolded DNA origami-based nanodevices, reconfigurable grid-like crystalline structures were successfully constructed using a scaffold-free approach by dictating the branching orientations of their constituent multi-way junctions—achieved via controlling the length of the inter-edge duplexes.[39,40] These pioneering studies opened the way for DNA nanodevices exhibiting more complex and controllable motions, toward which operations of the distinct movable joints in a combinatorial, sequential, and reversible manner are further desired.

In this study, we designed multiple controllable links in a single DNA origami to produce a multi-reconfigurable nanolattice that can be transformed into a variety of different

Received: February 22, 2023
Revised: April 1, 2023
Accepted: April 13, 2023
Published: April 27, 2023

https://doi.org/10.1021/jacsau.3c00091
JACS Au 2023, 3, 1435−1442

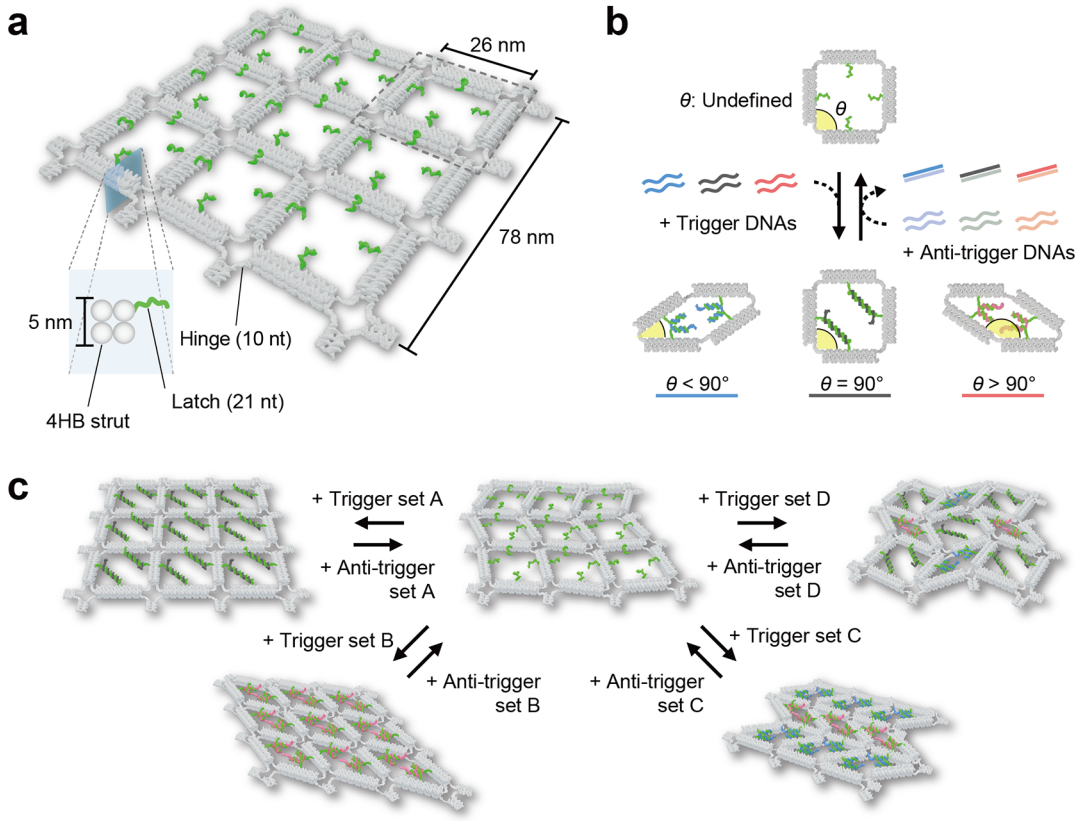

Figure 1. Design of a DNA origami nanolattice comprising shape-controllable nine frames. (a) Schematic representation of the DNA origami nanolattice. The latch DNA incorporated into the bundle is shown in green. (b) Schematic representation of the transformation mechanism of a frame [dashed box in (a)]. One pair of trigger DNAs is used to fix a $\theta = 90°$ square. A trigger DNA specifically binds the exposed ends of the latch DNA to face each other, acting as a sticking rod for the struts (dark gray strands). The other two pairs of trigger DNAs are used to fix a $\theta < 90°$ or >90° rhombus via specifically bringing the attached struts closer together (blue or red strands). (c) Transformation of the nanolattice from one shape into another by switching the set of trigger/anti-trigger DNAs.

shapes in a programmable manner depending on the combination of orthogonal input DNA signals. The modular and scalable link design allowed not only reversible reconfiguration but also sequential reconfiguration from one shape into another via an isothermal toehold-mediated strand displacement (TMSD) reaction.

RESULTS AND DISCUSSION

Nanolattice Design

Our DNA origami nanolattice is folded from a single-stranded M13mp18 scaffold DNA and is constructed as a 3 × 3 lattice (Figure 1a, see also Figures S1 and S2). Each frame of the nanolattice comprised four rigid four-helix bundles (4HBs), four flexible 10 nt ssDNA joints connecting the rigid struts, and four latch DNAs, each of which protruded from each 4HB. Reconfiguration of the frame was achieved by dictating the angle between the struts with a set of signal DNAs—termed trigger DNAs. Each trigger DNA can bridge a pair of latch DNAs to suppress the flexible motion of the joints and hold the bundles at predetermined relative angles (θ in Figure 1b). Three orthogonal pairs of trigger DNAs were designed for the transformation of each frame into a right-angled rhombus ($\theta <$ 90°), left-angled rhombus ($\theta >$ 90°), or square ($\theta =$ 90°) (Figure 1b). Each trigger DNA has a toehold sequence and thus can be displaced from the frame by adding its fully complementary ssDNA (anti-trigger DNA) (Figure S3).

The shape of each of the nine frames was regulated by their respective pairs of trigger DNAs, enabling reconfiguration of the nanolattice into various shapes, the interconversions of which were achieved by the TMSD reaction (Figure 1c).

Transformation of the Nanolattice into Various Shapes

Given that each strut (i.e., the 4HBs) of the frame has three patterns of angular selectivity ($\theta <$ 90°, = 90°, or >90°) on the two-dimensional (2D) plane, there was a large number of possible configurations for the nanolattice. Exhaustive search after imposing $\theta_{ij} = 40$, 90, or 140° on the frame of ith row and jth column resulted in 87 possible configurations. These values were estimated based on the length of one trigger DNA and the distance between one latch DNA and one joint. By excluding mirror-image configurations and rotationally symmetric configurations, there remained 17 types of configurations as apparently distinguishable on the 2D-plane (Figure S4).

We first investigated whether these 17 variations could be achieved by the addition of the corresponding set of trigger DNAs (Figure 2a). For this objective, the unfixed, flexible nanolattice was prepared by one-pot annealing of M13 scaffold DNA and staple strands following the removal of excess ssDNA strands (Figure S5). Aliquots of the purified sample were then allowed to react with the respective sets of trigger DNAs to produce the 17 different shapes (NL1−NL17) (Figure 2a, see also Figure S6). Atomic force microscopy (AFM) images before and after the addition of trigger DNAs

https://doi.org/10.1021/jacsau.3c00091
JACS Au 2023, 3, 1435−1442

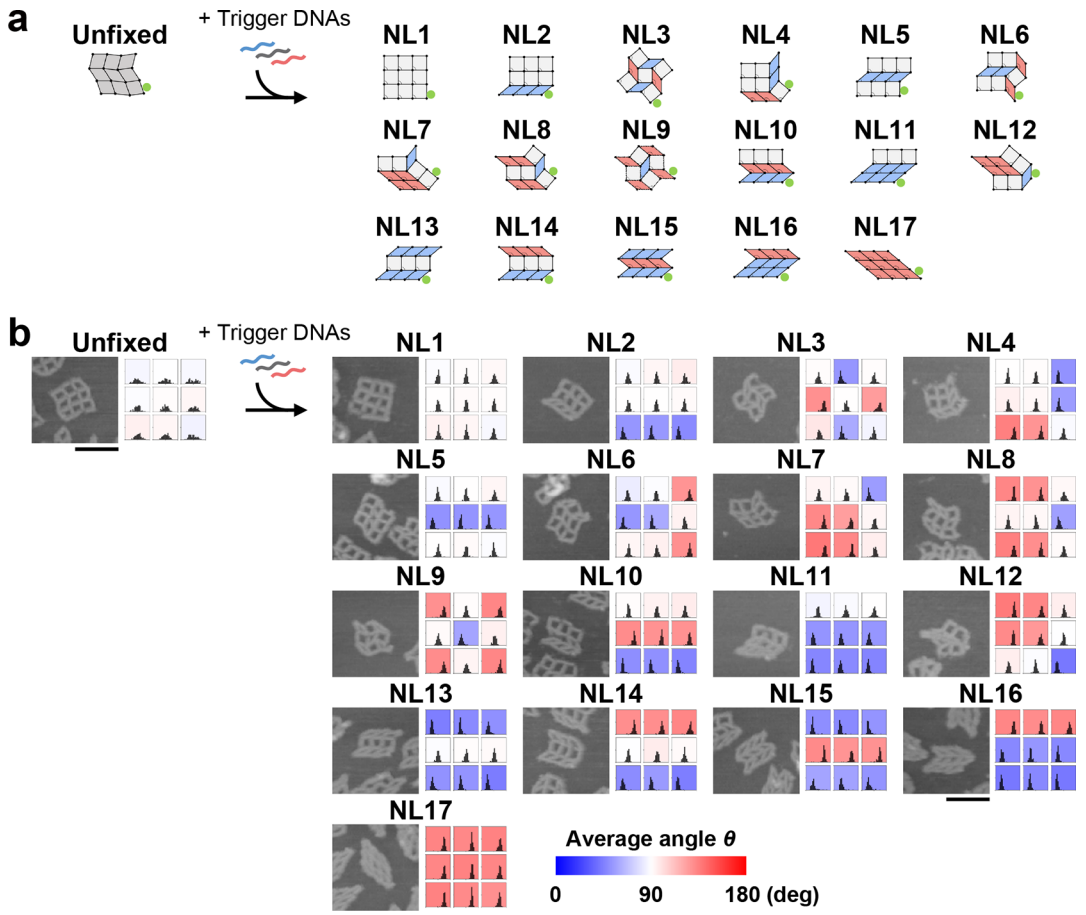

Figure 2. AFM analysis of the reconfiguration into 17 possible shapes using respective sets of trigger DNAs. (a) Schematic diagram of the reconfiguration from an unfixed shape into various shapes. (b) Cropped AFM images and histograms of angler distributions. The positions of the nine histograms correspond to the coordinates of each frame in the nanolattice. The background of the histograms was colored based on the average value of θ_{ij} according to a blue-to-red color map. Scale bar: 100 nm. $N > 100$. See also Figures S7–S9 for details.

showed that the unfixed nanolattice adopted various shapes, whereas those after the reaction exhibited one distinct shape (Figure 2b, see also Figures S7 and S8).

To quantify whether the nanolattice underwent the signal-set-specific transformation, θ_{ij} for individual nanolattices were measured, and their distributions were summarized in nine (3 × 3) histograms according to their positions (Figure S7). The orientation of the nanolattice on a substrate surface was distinguished by decorating one of the struts of a specific frame with streptavidin (Figures S1 and S7). Each frame of the unfixed nanolattice had an average angle of approximately 90°, yet exhibited wide angle distribution with a large standard deviation, reflecting its flexible and polymorphic nature. Following the reaction with trigger DNAs, the angle distribution for each frame became sharper, and the average angle matched with the target shape (Figure 2b, see also Figures S8 and S9). This was applicable in all 17 cases, demonstrating the selective transformation of our nanolattice into the target shape using the specific set of trigger DNAs.

Sequential Reconfiguration of the Nanolattice

To test the reconfigurability of the nanolattice, the unfixed nanolattice was allowed to react with the specific set of trigger/anti-trigger DNAs required to produce a square (NL1), cross (NL3), zigzag (NL15), or rhombus (NL17) shape. By sequentially treating the sample with the same or different set of trigger DNAs and their corresponding sets of anti-trigger DNAs in order, the transformation was cycled for two rounds. We tested $4^2 = 16$ possible pathways, 12 of which include reconfiguration from a particular shape into others. A sample solution of unfixed nanolattice was first prepared (stage 1) and then allowed to react with the first set of trigger DNAs (stage 2), in the same manner as presented in Figure 2. Subsequently, the corresponding set of anti-trigger DNAs against the first set of trigger DNAs was added to induce the reverse transformation (stage 3). After the reaction, the second set of trigger DNAs was added to induce the second transformation (stage 4), and finally, the second set of anti-trigger DNAs (stage 5) was added to unfix the nanolattice again. Reactions at stages 2–4 were conducted at 37 °C for 6 h. After the reaction at each stage, the nanolattice sample was imaged by AFM in solution to analyze the changes in its apparent shape.

Figure 3 summarizes the representative AFM images after each stage and the results of the statistical analysis of θ_{ij}. In all pathways, the nanolattices after stages 2 and 4 assumed expected configurations with average values of θ_{ij} that matched with the target shapes, whereas those after stages 1, 3, and 5 assumed indeterminate shapes with wide distributions of θ_{ij} (Figure 3, see also Figures S10 and S11), suggesting the success of repeated transformation into a selected shape and programmable reconfiguration from one shape to another.

https://doi.org/10.1021/jacsau.3c00091
JACS Au 2023, 3, 1435–1442

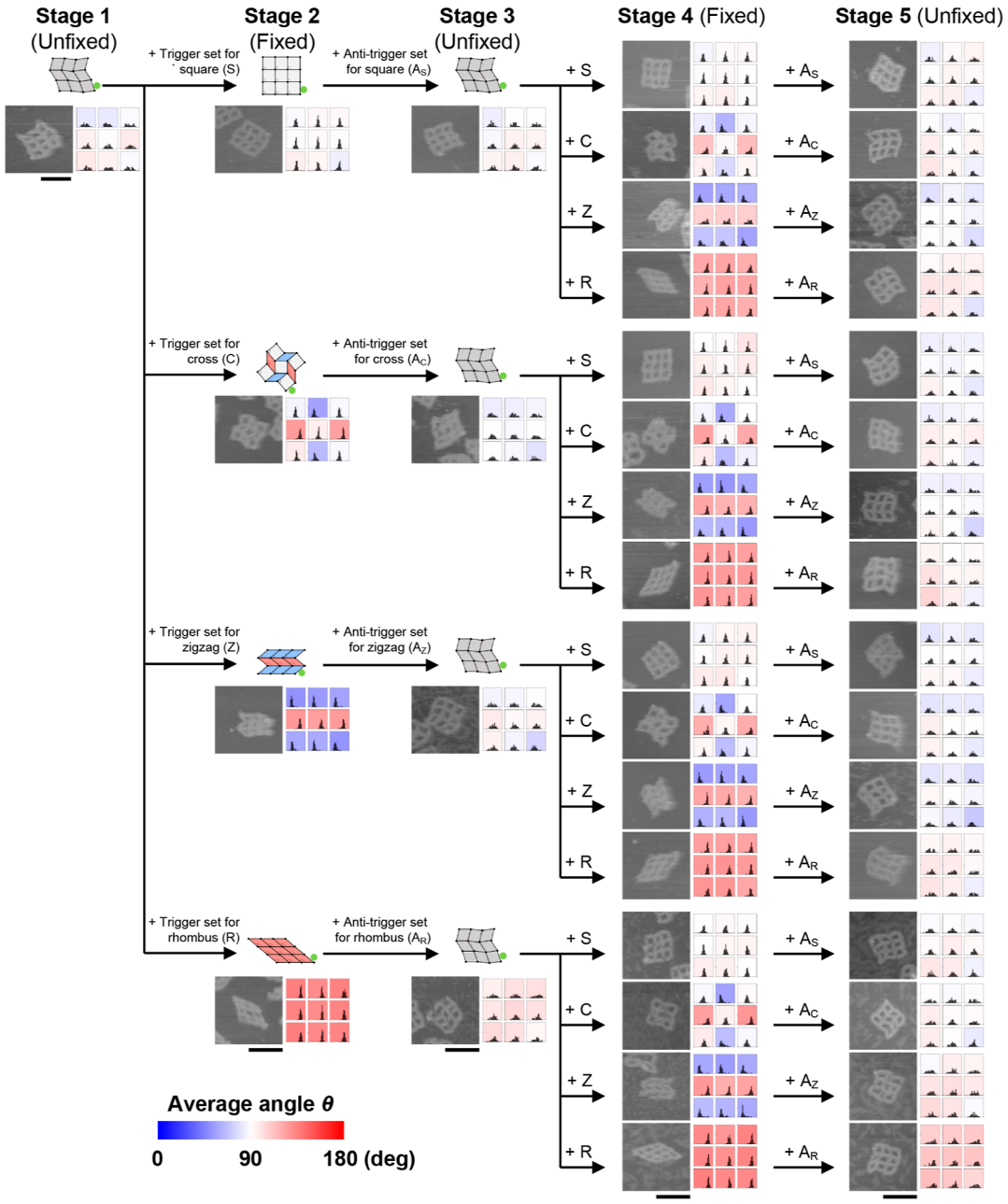

Figure 3. Repeated and sequential reconfiguration of the nanolattice by adding the corresponding set of trigger/anti-trigger DNAs in order. Flow of the reconfiguration from stages 1 to 5 is summarized together with representative AFM images and histograms of angler distributions at each stage. Unfixed nanolattice was reconfigured into NL1, NL3, NL15, or NL17 (from top to bottom) at stage 2 and further reconfigured into NL1, NL3, NL15, and NL17 at stage 4. Scale bar: 100 nm. $N > 90$ for each stage. See also Figures S10 and S11 for details.

Hierarchical Self-Assembly into 7 × 7 Nanolattice and Its Reconfiguration

Our design approach should, in principle, be scalable into larger, higher-order structures. To test this idea, we redesigned the nanolattice structure such that its heterotetramerization results in the formation of a 7 × 7 lattice (Figure 4a, see also Figure S12). Half-struts at the connection ends of each monomer were designed to make complete struts upon the multimerization, resulting in the additional frames. Each monomer was first prepared as a 3 × 3 square lattice by annealing scaffold DNA and staple strands with trigger DNAs that were required to fix the angles θ between 4HBs at 90°. Pairs of monomers (A1 and B1 or A2 and B2) were then mixed at an equimolar ratio to produce 7 × 3 lattices, which were further assembled into a 7 × 7 lattice (Figure 4a).

The formation of the target products in each step of the hierarchical assembly was addressed by agarose gel electrophoresis (AGE). As shown in Figure 4b, two different heterodimers (A1-B1 and A2-B2) were successfully prepared, as evidenced by the decrease of monomer bands and clear band shifts. Their assembly into the heterotetramer was also evidenced by the disappearance of the A1-B1 and A2-B2 bands and further band shifts after the second step. AFM images of the tetrameric sample revealed the successful construction of the scaled-up, 7 × 7 lattice (Figure 4c, left).

The 7 × 7 lattice was then subjected to the reconfiguration. The anti-trigger DNAs were first added to remove the pre-

https://doi.org/10.1021/jacsau.3c00091
JACS Au 2023, 3, 1435−1442

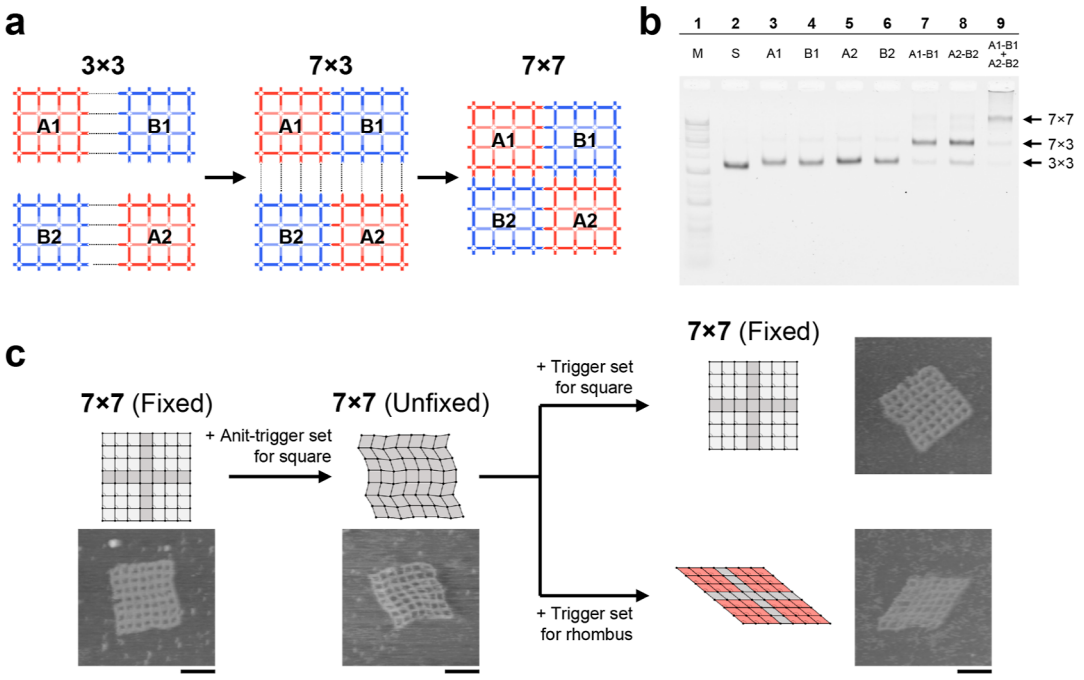

Figure 4. Hierarchical construction of the tetramer of the DNA origami nanolattice and its signal-dependent reconfiguration. (a) Schematic illustration of the hierarchical assembly of the 7 × 7 nanolattice. (b) Agarose gel electrophoresis analysis of the 7 × 7 nanolattice assembly. Lane 1: ladder maker, lane 2: scaffold DNA, lane 3: A1 3 × 3 nanolattice, lane 4: B1 3 × 3 nanolattice, lane 5: A2 3 × 3 nanolattice, lane 6: B2 3 × 3 nanolattice, lane 7: A1-B1 7 × 3 nanolattice, lane 8: A2-B2 7 × 3 nanolattice, and lane 9: 7 × 7 nanolattice consisting of two types of 7 × 3 nanolattices. (c) Schematic illustrations of signal DNA-induced reconfiguration of the 7 × 7 nanolattice. Representative AFM images at each stage are shown. Scale bar: 100 nm.

incorporated trigger DNAs and make the lattice "unfixed" (Figure 4c, middle). Next, the unfixed 7 × 7 lattice was reversed into the 7 × 7 square lattice or reconfigured into the 7 × 7 rhombus by adding the corresponding set of trigger DNAs (Figure 4c, right). Representative AFM images of the sample after each step (Figure S13) revealed the transformation of the 7 × 7 lattice into the desired shape, which also demonstrates the scalability of our design.

CONCLUSIONS

In this study, we demonstrated the programmable reconfiguration of a DNA origami nanolattice via a TMSD reaction. Generally, the construction of multiple structural variations from a single DNA origami design requires the replacement of a large number of staple strands because even slight changes in the path of the scaffold strand can cause the revision of almost all staple sequences.[12,41] This costly preparation has been challenged by the "module-based" design approach, which enables the construction of a series of DNA nanostructures with different morphologies from a single DNA origami design merely by replacing individual parts of staple strands.[42−47] In our design, each frame can be regarded as a module, the cumulative reconfiguration of which determines the overall shape. This modular design enabled a variety of configurations of the nanolattice by dictating a target shape with a combination of 18 trigger DNAs, which corresponds to approximately 8% of the total staple strands only. Furthermore, by replacing the incorporated set of the trigger DNAs with another via an isothermal TMSD reaction, the structural shapes could be repeatedly and sequentially reconfigured.

Given that the properties and functions of material are tightly dependent on its molecular composition as well as the arrangement of its constituent molecules, a platform enabling manipulation of the relative positions and postures of multiple molecules with nanoscale precision can be expected to lead to the development of novel materials whose functions can be switched arbitrarily on demand. Owing to their surface addressability, DNA nanostructures have been utilized as scaffolds for organizing a variety of molecules, such as inorganic nanoparticles,[48,49] nucleic acids,[50,51] and proteins.[52−56] Dynamic nanostructures, such as DNA tweezers, capable of open/close motion have also been used to control the distance between a pair of enzyme and its cofactor.[57] Modularity of the frame in our dynamic nanolattice should allow its surface decoration with multiple, possibly even different, molecules and their rearrangement along with the reconfiguration of the lattice. In addition, the reconfiguration could be operated at physiologically relevant temperatures (i.e., 37 °C), ensuring protection of biomolecules from thermal denaturation. Coupled with its scalability, our design approach paves the way for constructing more complex nanosystems whose properties and functions can be controlled in a programmable manner.[58]

MATERIALS AND METHODS

Preparation of DNA Origami Structures

All staple strands were purchased from Eurofins Genomics Tokyo (Tokyo, Japan). Single-stranded M13mp18 viral DNA and cyclic ssDNA of 8064 nt (p8064) were purchased from Tilibit Nanosystems (Garching, Germany). DNA origami structures were designed using caDNAno software[59] for strand routing. Assembly of the origami structures was accomplished by mixing 10−40 nM scaffold DNA (M13mp18 ssDNA or p8064) with staple strands in 20−100 μL of the folding buffer containing 5 mM Tris−HCl (pH 8.0), 1 mM EDTA, and 15 mM $MgCl_2$. The mixture was incubated at 85 °C for 5 min, annealed by sequentially reducing the temperature from 85 to 65

https://doi.org/10.1021/jacsau.3c00091
JACS Au 2023, 3, 1435−1442

°C at a rate of −1 °C/min, then incubated at 65 °C for 15 min, reducing the temperature from 65 to 15 °C at a rate of −0.5 °C/min, and finally incubated at 15 °C.

Purification of DNA Origami by Density Gradient Centrifugation

The assembled DNA origami structure was purified using a glycerol gradient method.[60] To prepare a linear glycerol gradient (5−45%, v/v), nine layers (200 μL per layer) of glycerol solution in 1 × TE-Mg buffer (5 mM Tris−HCl [pH 8.0], 15 mM $MgCl_2$, and 1 mM EDTA) were carefully added into a 2.2 mL ultracentrifuge tube with 5% concentration decrement per layer, starting with a 45% glycerol solution at the bottom. The tube was incubated overnight at 25 °C to prepare a glycerol gradient. A solution of DNA origami nanostructures (200 μL) containing 5% glycerol was then loaded on top of the glycerol gradient. The tube was then centrifuged at 50,000 rpm (214,288*g*) for 1 h at 4 °C using an ultracentrifuge (himac CS150GXII, Hitachi, Tokyo, Japan) equipped with a swing-rotor (S55S-2017, Hitachi, Tokyo, Japan). After centrifugation, 14 fractions (750 μL × 1, 75 μL × 12, and 350 μL × 1) were collected sequentially from the top to bottom of the tube. Aliquots of each fraction were subjected to AGE (Figure S5a). The fractions exhibiting the target bands were mixed and concentrated using Amicon Ultra-0.5 mL centrifugal filters (MWCO 100 kDa) (Merck KGaA, Darmstadt, Germany). The glycerol-containing buffer was also replaced with glycerol-free buffer during ultracentrifugation. The concentration of the purified sample was determined by quantifying the band intensity of the origami structures before and after purification by AGE (Figure S5b).

Agarose Gel Electrophoresis

The samples were loaded for electrophoresis on a 1.5% agarose gel containing 5 mM $MgCl_2$ in a 0.5× Tris-borate-EDTA buffer solution under 100 V at 4 °C. The gels were then imaged with ChemiDOC MP (Bio-Rad Laboratories, Inc. Hercules, CA) using SYBR Gold Nucleic Acid Gel Stain (Thermo Fisher Scientific, Waltham, MA) as the staining dye.

Atomic Force Microscopy

AFM imaging was performed using tip scan high-speed AFM (BIXAM, Olympus, Tokyo, Japan), which was improved based on a previously developed prototype AFM[61] in a solution of observation buffer containing 5 mM Tris−HCl (pH 8.0), 15 mM $MgCl_2$, and 1 mM EDTA. A 2 μL drop of the 1−3 nM sample in the observation buffer was deposited onto a freshly cleaved mica surface (φ 3.0 mm) and incubated for 1 min, followed by a 1 μL drop of 0.1% 3-aminopropyltriethoxysilane and incubated for 3 min. Small cantilevers (9 μm long, 2 μm wide, and 130 nm thick) with a spring constant of 0.1 N/m (USC−F0.8-k0.1-T12; Nanoworld, Neuchâtel, Switzerland) were used to scan the sample surface. The 320 × 240 pixel images were collected at a scan line rate of 0.5 frames per sec. The imaged sequences were analyzed using ImageJ software (http://imagej.nih.gov/ij/). The broken or aggregated structures were not used in analysis.

Transformation of a Nanolattice

A sample solution of the purified unfixed nanolattice was first prepared (stage 1) and then allowed to react with first trigger DNAs at the molar ratio of nanolattice/each first trigger DNA = 1:2 (stage 2). Next, a set of first anti-trigger DNAs was added at the molar ratio of nanolattice/each first anti-trigger DNA = 1:4, to remove the corresponding trigger DNAs (stage 3). Subsequently, six-folds of second trigger DNAs were added to induce second transformation (stage 4), and finally eight-folds of second anti-trigger DNAs (stage 5) were added to unfix the nanolattice again. The concentrations of the nanolattice at stages 1, 2, 3, 4, and 5 were ∼20, ∼15, ∼12, ∼10, and ∼5 nM, respectively. Reactions at stages 2−4 were conducted at 37 °C for 6 h. Before AFM observation, the lattice was allowed to react with 100 equimolar concentration of streptavidin (FUJIFILM Wako Pure Chemical, Osaka, Japan) for specific labeling as an orientation marker.

Preparation of 7 × 3 or 7 × 7 Nanolattices

Four types of 3 × 3 nanolattices with extended terminal edges were designed (A1, A2, B1, and B2) to construct a 7 × 7 nanolattice through the heterotetramerization. Each 3 × 3 nanolattice was assembled by mixing and annealing the scaffold strand (p8064), staple strand, and a set of trigger DNAs that fixes all frames in a square. Next, 7 × 3 nanolattices were constructed by mixing purified A1 and B1 (or A2 and B2) at the same molar ratio (final concentration of ∼20 nM). Finally, a 7 × 7 nanolattice was constructed by mixing A1-B1 and A2-B2 7 × 3 nanolattices (final concentration of ∼10 nM) at the same molar ratio. To make the 7 × 7 nanolattice transformable, anti-trigger DNAs were first added at the molar ratio of nanolattice/each anti-trigger DNA = 1:2, to remove the pre-incorporated trigger DNAs (final concentration of ∼15 nM). After that, a set of trigger DNAs was added at the molar ratio of nanolattice/each trigger DNA = 1:4, to induce the transformation (final concentration of ∼10 nM). Each reaction was carried out at 37 °C for 6 h.

■ ASSOCIATED CONTENT

Supporting Information

The Supporting Information is available free of charge at https://pubs.acs.org/doi/10.1021/jacsau.3c00091.

Structural designs of DNA origami nanolattices; routing of scaffold DNA; AGE results after density gradient centrifugation; large-area AFM images; AFM image analyses; and designs and sequences of staple DNAs, trigger DNAs, and anti-trigger DNAs (PDF)

■ AUTHOR INFORMATION

Corresponding Author

Yuki Suzuki − *Frontier Research Institute for Interdisciplinary Sciences, Tohoku University, Sendai 980-8578, Japan; Department of Chemistry for Materials, Graduate School of Engineering, Mie University, Tsu 514-8507, Japan;* orcid.org/0000-0003-1848-0105; Email: ysuzuki@chem.mie-u.ac.jp

Authors

Kotaro Watanabe − *Department of Robotics, Graduate School of Engineering, Tohoku University, Sendai 980-8579, Japan*

Ibuki Kawamata − *Department of Robotics, Graduate School of Engineering, Tohoku University, Sendai 980-8579, Japan;* orcid.org/0000-0002-1955-8827

Satoshi Murata − *Department of Robotics, Graduate School of Engineering, Tohoku University, Sendai 980-8579, Japan*

Complete contact information is available at: https://pubs.acs.org/10.1021/jacsau.3c00091

Author Contributions

K.W., I.K., S.M., and Y.S. conceived the study. K.W. and Y.S. designed experiments and analyses. K.W. conducted biochemical experiments. K.W. and Y.S. conducted AFM imaging. K.W. performed image analyses. All authors were involved in the discussion of results and comments on the manuscript. CRediT: **Kotaro Watanabe** conceptualization, data curation, formal analysis, investigation, methodology, validation, writing-original draft, writing-review & editing; **Ibuki Kawamata** conceptualization, validation, writing-review & editing; **Satoshi Murata** conceptualization, funding acquisition, project administration, supervision, writing-review & editing; **Yuki Suzuki** conceptualization, data curation, funding acquisition, investigation, methodology, project administration, supervision,

https://doi.org/10.1021/jacsau.3c00091
JACS Au 2023, 3, 1435−1442

validation, visualization, writing-original draft, writing-review & editing.

Funding

This work was supported by the Japan Society for the Promotion of Science (JSPS) Grant-in-Aid for Scientific Research (KAKENHI; grant numbers 19H04201, 21H05864, 22K05686, and 22H03682 to Y.S.; 20H05971 and 22K12255 to I.K.; and 20K20979 and 20H05969 to S.M.).

Notes

The authors declare no competing financial interest.

■ ACKNOWLEDGMENTS

Y.S. would like to thank Eriko Mano and Nobuaki Sakai for technical assistance.

■ ABBREVATION

ssDNA	single-stranded DNA
dsDNA	double-stranded DNA
TMSD	toehold-mediated strand displacement
4HB	four-helix bundle
AFM	atomic force microscopy

■ REFERENCES

(1) Seeman, N. C. DNA in a material world. *Nature* **2003**, *421*, 427−431.
(2) Seeman, N. C.; Sleiman, H. F. DNA nanotechnology. *Nat. Rev. Mater.* **2017**, *3*, 17068.
(3) Chen, J. H.; Seeman, N. C. Synthesis from DNA of a molecule with the connectivity of a cube. *Nature* **1991**, *350*, 631−633.
(4) Mao, C.; Sun, W.; Seeman, N. C. Assembly of Borromean rings from DNA. *Nature* **1997**, *386*, 137−138.
(5) Winfree, E.; Liu, F.; Wenzler, L. A.; Seeman, N. C. Design and self-assembly of two-dimensional DNA crystals. *Nature* **1998**, *394*, 539−544.
(6) Ijas, H.; Nummelin, S.; Shen, B.; Kostiainen, M. A.; Linko, V. Dynamic DNA Origami Devices: from Strand-Displacement Reactions to External-Stimuli Responsive Systems. *Int. J. Mol. Sci.* **2018**, *19*, 2114.
(7) Yurke, B.; Turberfield, A. J.; Mills, A. P., Jr.; Simmel, F. C.; Neumann, J. L. A DNA-fuelled molecular machine made of DNA. *Nature* **2000**, *406*, 605−608.
(8) Marko, J. F.; Siggia, E. D. Stretching DNA. *Macromolecules* **1995**, *28*, 8759−8770.
(9) Smith, S. B.; Cui, Y.; Bustamante, C. Overstretching B-DNA: the elastic response of individual double-stranded and single-stranded DNA molecules. *Science* **1996**, *271*, 795−799.
(10) Manning, G. S. The persistence length of DNA is reached from the persistence length of its null isomer through an internal electrostatic stretching force. *Biophys. J.* **2006**, *91*, 3607−3616.
(11) Rothemund, P. W. Folding DNA to create nanoscale shapes and patterns. *Nature* **2006**, *440*, 297−302.
(12) Dietz, H.; Douglas, S. M.; Shih, W. M. Folding DNA into twisted and curved nanoscale shapes. *Science* **2009**, *325*, 725−730.
(13) Douglas, S. M.; Dietz, H.; Liedl, T.; Hogberg, B.; Graf, F.; Shih, W. M. Self-assembly of DNA into nanoscale three-dimensional shapes. *Nature* **2009**, *459*, 414−418.
(14) Han, D.; Pal, S.; Nangreave, J.; Deng, Z.; Liu, Y.; Yan, H. DNA origami with complex curvatures in three-dimensional space. *Science* **2011**, *332*, 342−346.
(15) Marras, A. E.; Zhou, L.; Su, H. J.; Castro, C. E. Programmable motion of DNA origami mechanisms. *Proc. Natl. Acad. Sci. U.S.A.* **2015**, *112*, 713−718.
(16) Nummelin, S.; Shen, B.; Piskunen, P.; Liu, Q.; Kostiainen, M. A.; Linko, V. Robotic DNA Nanostructures. *ACS Synth. Biol.* **2020**, *9*, 1923−1940.
(17) Mills, A.; Aissaoui, N.; Finkel, J.; Elezgaray, J.; Bellot, G. Mechanical DNA Origami to Investigate Biological Systems. *Adv. Biol.* **2022**, *7*, No. e2200224.
(18) Andersen, E. S.; Dong, M.; Nielsen, M. M.; Jahn, K.; Subramani, R.; Mamdouh, W.; Golas, M. M.; Sander, B.; Stark, H.; Oliveira, C. L.; Pedersen, J. S.; Birkedal, V.; Besenbacher, F.; Gothelf, K. V.; Kjems, J. Self-assembly of a nanoscale DNA box with a controllable lid. *Nature* **2009**, *459*, 73−76.
(19) Kuzuya, A.; Sakai, Y.; Yamazaki, T.; Xu, Y.; Komiyama, M. Nanomechanical DNA origami 'single-molecule beacons' directly imaged by atomic force microscopy. *Nat. Commun.* **2011**, *2*, 449.
(20) Douglas, S. M.; Bachelet, I.; Church, G. M. A logic-gated nanorobot for targeted transport of molecular payloads. *Science* **2012**, *335*, 831−834.
(21) Gerling, T.; Wagenbauer, K. F.; Neuner, A. M.; Dietz, H. Dynamic DNA devices and assemblies formed by shape-complementary, non-base pairing 3D components. *Science* **2015**, *347*, 1446−1452.
(22) Kroener, F.; Heerwig, A.; Kaiser, W.; Mertig, M.; Rant, U. Electrical Actuation of a DNA Origami Nanolever on an Electrode. *J. Am. Chem. Soc.* **2017**, *139*, 16510−16513.
(23) Willner, E. M.; Kamada, Y.; Suzuki, Y.; Emura, T.; Hidaka, K.; Dietz, H.; Sugiyama, H.; Endo, M. Single-Molecule Observation of the Photoregulated Conformational Dynamics of DNA Origami Nanoscissors. *Angew. Chem., Int. Ed.* **2017**, *56*, 15324−15328.
(24) Takenaka, T.; Endo, M.; Suzuki, Y.; Yang, Y.; Emura, T.; Hidaka, K.; Kato, T.; Miyata, T.; Namba, K.; Sugiyama, H. Photoresponsive DNA nanocapsule having an open/close system for capture and release of nanomaterials. *Chem. Eur. J.* **2014**, *20*, 14951−14954.
(25) Ijas, H.; Hakaste, I.; Shen, B.; Kostiainen, M. A.; Linko, V. Reconfigurable DNA Origami Nanocapsule for pH-Controlled Encapsulation and Display of Cargo. *ACS Nano* **2019**, *13*, 5959−5967.
(26) Powell, J. T.; Akhuetie-Oni, B. O.; Zhang, Z.; Lin, C. DNA Origami Rotaxanes: Tailored Synthesis and Controlled Structure Switching. *Angew. Chem., Int. Ed.* **2016**, *55*, 11412−11416.
(27) Mills, A.; Aissaoui, N.; Maurel, D.; Elezgaray, J.; Morvan, F.; Vasseur, J. J.; Margeat, E.; Quast, R. B.; Lai Kee-Him, J.; Saint, N.; Benistant, C.; Nord, A.; Pedaci, F.; Bellot, G. A modular spring-loaded actuator for mechanical activation of membrane proteins. *Nat. Commun.* **2022**, *13*, 3182.
(28) Ketterer, P.; Willner, E. M.; Dietz, H. Nanoscale rotary apparatus formed from tight-fitting 3D DNA components. *Sci. Adv.* **2016**, *2*, No. e1501209.
(29) Tomaru, T.; Suzuki, Y.; Kawamata, I.; Nomura, S. i. M.; Murata, S. Stepping operation of a rotary DNA origami device. *Chem. Commun.* **2017**, *53*, 7716−7719.
(30) Yang, Y.; Tashiro, R.; Suzuki, Y.; Emura, T.; Hidaka, K.; Sugiyama, H.; Endo, M. A Photoregulated DNA-Based Rotary System and Direct Observation of Its Rotational Movement. *Chem. Eur. J.* **2017**, *23*, 3979−3985.
(31) Kopperger, E.; List, J.; Madhira, S.; Rothfischer, F.; Lamb, D. C.; Simmel, F. C. A self-assembled nanoscale robotic arm controlled by electric fields. *Science* **2018**, *359*, 296−301.
(32) Lauback, S.; Mattioli, K. R.; Marras, A. E.; Armstrong, M.; Rudibaugh, T. P.; Sooryakumar, R.; Castro, C. E. Real-time magnetic actuation of DNA nanodevices via modular integration with stiff micro-levers. *Nat. Commun.* **2018**, *9*, 1446.
(33) Pumm, A. K.; Engelen, W.; Kopperger, E.; Isensee, J.; Vogt, M.; Kozina, V.; Kube, M.; Honemann, M. N.; Bertosin, E.; Langecker, M.; Golestanian, R.; Simmel, F. C.; Dietz, H. A DNA origami rotary ratchet motor. *Nature* **2022**, *607*, 492−498.
(34) Funke, J. J.; Dietz, H. Placing molecules with Bohr radius resolution using DNA origami. *Nat. Nanotechnol.* **2016**, *11*, 47−52.
(35) Han, D.; Pal, S.; Yang, Y.; Jiang, S.; Nangreave, J.; Liu, Y.; Yan, H. DNA gridiron nanostructures based on four-arm junctions. *Science* **2013**, *339*, 1412−1415.

https://doi.org/10.1021/jacsau.3c00091
JACS Au 2023, 3, 1435−1442

(36) Zhou, L.; Marras, A. E.; Huang, C. M.; Castro, C. E.; Su, H. J. Paper Origami-Inspired Design and Actuation of DNA Nanomachines with Complex Motions. *Small* **2018**, *14*, No. e1802580.
(37) Huang, C. M.; Kucinic, A.; Le, J. V.; Castro, C. E.; Su, H. J. Uncertainty quantification of a DNA origami mechanism using a coarse-grained model and kinematic variance analysis. *Nanoscale* **2019**, *11*, 1647−1660.
(38) Ke, Y.; Meyer, T.; Shih, W. M.; Bellot, G. Regulation at a distance of biomolecular interactions using a DNA origami nanoactuator. *Nat. Commun.* **2016**, *7*, 10935.
(39) Liu, L.; Li, Z.; Li, Y.; Mao, C. Rational Design and Self-Assembly of Two-Dimensional, Dodecagonal DNA Quasicrystals. *J. Am. Chem. Soc.* **2019**, *141*, 4248−4251.
(40) Wang, W.; Chen, C.; Vecchioni, S.; Zhang, T.; Wu, C.; Ohayon, Y. P.; Sha, R.; Seeman, N. C.; Wei, B. Reconfigurable Two-Dimensional DNA Lattices: Static and Dynamic Angle Control. *Angew. Chem., Int. Ed.* **2021**, *60*, 25781−25786.
(41) Zhou, L.; Marras, A. E.; Su, H. J.; Castro, C. E. DNA origami compliant nanostructures with tunable mechanical properties. *ACS Nano* **2014**, *8*, 27−34.
(42) Lee, C.; Lee, J. Y.; Kim, D. N. Polymorphic design of DNA origami structures through mechanical control of modular components. *Nat. Commun.* **2017**, *8*, 2067.
(43) Pfeifer, W.; Lill, P.; Gatsogiannis, C.; Sacca, B. Hierarchical Assembly of DNA Filaments with Designer Elastic Properties. *ACS Nano* **2018**, *12*, 44−55.
(44) Suzuki, Y.; Kawamata, I.; Mizuno, K.; Murata, S. Large Deformation of a DNA-Origami Nanoarm Induced by the Cumulative Actuation of Tension-Adjustable Modules. *Angew. Chem., Int. Ed.* **2020**, *132*, 6289−6293.
(45) Karna, D.; Stilgenbauer, M.; Jonchhe, S.; Ankai, K.; Kawamata, I.; Cui, Y.; Zheng, Y. R.; Suzuki, Y.; Mao, H. Chemo-Mechanical Modulation of Cell Motions Using DNA Nanosprings. *Bioconjug. Chem.* **2021**, *32*, 311−317.
(46) Wang, D.; Yu, L.; Huang, C. M.; Arya, G.; Chang, S.; Ke, Y. Programmable Transformations of DNA Origami Made of Small Modular Dynamic Units. *J. Am. Chem. Soc.* **2021**, *143*, 2256−2263.
(47) Liu, Y.; Cheng, J.; Fan, S.; Ge, H.; Luo, T.; Tang, L.; Ji, B.; Zhang, C.; Cui, D.; Ke, Y.; Song, J. Modular Reconfigurable DNA Origami: From Two-Dimensional to Three-Dimensional Structures. *Angew. Chem., Int. Ed.* **2020**, *59*, 23277−23282.
(48) Kuzyk, A.; Schreiber, R.; Fan, Z.; Pardatscher, G.; Roller, E. M.; Hogele, A.; Simmel, F. C.; Govorov, A. O.; Liedl, T. DNA-based self-assembly of chiral plasmonic nanostructures with tailored optical response. *Nature* **2012**, *483*, 311−314.
(49) Schreiber, R.; Do, J.; Roller, E. M.; Zhang, T.; Schuller, V. J.; Nickels, P. C.; Feldmann, J.; Liedl, T. Hierarchical assembly of metal nanoparticles, quantum dots and organic dyes using DNA origami scaffolds. *Nat. Nanotechnol.* **2014**, *9*, 74−78.
(50) Gu, H.; Chao, J.; Xiao, S. J.; Seeman, N. C. A proximity-based programmable DNA nanoscale assembly line. *Nature* **2010**, *465*, 202−205.
(51) Wickham, S. F.; Endo, M.; Katsuda, Y.; Hidaka, K.; Bath, J.; Sugiyama, H.; Turberfield, A. J. Direct observation of stepwise movement of a synthetic molecular transporter. *Nat. Nanotechnol.* **2011**, *6*, 166−169.
(52) Voigt, N. V.; Torring, T.; Rotaru, A.; Jacobsen, M. F.; Ravnsbaek, J. B.; Subramani, R.; Mamdouh, W.; Kjems, J.; Mokhir, A.; Besenbacher, F.; Gothelf, K. V. Single-molecule chemical reactions on DNA origami. *Nat. Nanotechnol.* **2010**, *5*, 200−203.
(53) Fu, J.; Liu, M.; Liu, Y.; Woodbury, N. W.; Yan, H. Interenzyme substrate diffusion for an enzyme cascade organized on spatially addressable DNA nanostructures. *J. Am. Chem. Soc.* **2012**, *134*, 5516−5519.
(54) Ngo, T. A.; Nakata, E.; Saimura, M.; Morii, T. Spatially Organized Enzymes Drive Cofactor-Coupled Cascade Reactions. *J. Am. Chem. Soc.* **2016**, *138*, 3012−3021.
(55) Ke, G.; Liu, M.; Jiang, S.; Qi, X.; Yang, Y. R.; Wootten, S.; Zhang, F.; Zhu, Z.; Liu, Y.; Yang, C. J.; Yan, H. Directional Regulation of Enzyme Pathways through the Control of Substrate Channeling on a DNA Origami Scaffold. *Angew. Chem., Int. Ed.* **2016**, *55*, 7483−7486.
(56) Kahn, J. S.; Xiong, Y.; Huang, J.; Gang, O. Cascaded Enzyme Reactions over a Three-Dimensional, Wireframe DNA Origami Scaffold. *JACS Au* **2022**, *2*, 357−366.
(57) Liu, M.; Fu, J.; Hejesen, C.; Yang, Y.; Woodbury, N. W.; Gothelf, K.; Liu, Y.; Yan, H. A DNA tweezer-actuated enzyme nanoreactor. *Nat. Commun.* **2013**, *4*, 2127.
(58) Murata, S.; Toyota, T.; Nomura, S. M.; Nakakuki, T.; Kuzuya, A. Molecular Cybernetics: Challenges toward Cellular Chemical Artificial Intelligence. *Adv. Funct. Mater.* **2022**, *32*, 2201866.
(59) Douglas, S. M.; Marblestone, A. H.; Teerapittayanon, S.; Vazquez, A.; Church, G. M.; Shih, W. M. Rapid prototyping of 3D DNA-origami shapes with caDNAno. *Nucleic Acids Res.* **2009**, *37*, 5001−5006.
(60) Lin, C.; Perrault, S. D.; Kwak, M.; Graf, F.; Shih, W. M. Purification of DNA-origami nanostructures by rate-zonal centrifugation. *Nucleic Acids Res.* **2013**, *41*, No. e40.
(61) Suzuki, Y.; Sakai, N.; Yoshida, A.; Uekusa, Y.; Yagi, A.; Imaoka, Y.; Ito, S.; Karaki, K.; Takeyasu, K. High-speed atomic force microscopy combined with inverted optical microscopy for studying cellular events. *Sci. Rep.* **2013**, *3*, 2131.

NOTE ADDED AFTER ASAP PUBLICATION

This paper was published online April 27, 2023, with a drawing error in Figure 1. The corrected version reposted with the issue May 22, 2023.

https://doi.org/10.1021/jacsau.3c00091
JACS Au 2023, 3, 1435−1442